

Analysis of the Urban Heat Island Phenomenon in Chau Doc City, An Giang Province, Vietnam

Tran Thi Hong Ngoc¹, Nguyen Duc Thang² and Phan Truong Khanh^{3*}

^{1,3}Faculty of Engineering-Technology-Environment, An Giang University, Vietnamese National University, Ho Chi Minh City.

²Master student in Can Tho University, Vietnam

^{3*}ptkhanhagu@gmail.com

ABSTRACT

This study aims to evaluate the relationship between the Normalized Difference Vegetation Index (NDVI) and Land Surface Temperature (LST) in Chau Doc City, An Giang Province, during the period from 2014 to 2022, using remote sensing data and spatial analysis. The results reveal a significant inverse relationship between NDVI and LST, with the strongest correlation observed in 2018 ($R=0.687$), indicating the important role of vegetation in regulating urban temperature. However, by 2022, this correlation had declined markedly ($R=0.264$), reflecting a decrease in the cooling effectiveness of vegetation. Analysis of LST variations and thermal frequency maps shows that high-temperature zones are concentrated in the urban core and tend to expand into pier-urban areas. The study clearly identifies the increasing risk of urban heat island effects and proposes solutions such as green space planning, sustainable development management, and the application of remote sensing technology in urban thermal monitoring.
Keywords: NDVI; Land Surface Temperature; Remote Sensing; Spatial Analysis; Chau Doc.

1. INTRODUCTION

Urban space is a complex system comprising physical elements, human factors, and socio-economic activities that are closely interwoven, forming the unique structure and function of a city. The process of urbanization leads to profound changes in the natural landscape, resulting in alterations in land use patterns, building density, and surface material composition. These changes directly impact the urban microclimate. Specifically, the expansion of urban areas increases the coverage of concrete, asphalt, and other artificial materials with high heat absorption capacity, while reducing the areas of greenery and natural water bodies—key elements in regulating temperature and mitigating climate conditions (Oke, 1982; Arnfield, 2003).

The Urban Heat Island (UHI) phenomenon is defined as the difference in air temperature between urban areas and their surrounding suburban or rural regions, primarily caused by changes in surface structure, building density, and anthropogenic heat emissions (Voogt & Oke, 2003). Studies in major cities such as New York (Roth et al., 1989), Tokyo (Kimura & Kanda, 2006), and Singapore (Ng et al., 2012) have shown that high building density, lack of vegetation and water bodies, along with intense urban activity, contribute to increased surface and air temperatures within cities. Urban development driven by the need to accommodate growing populations has led to increased waste heat from human activities, thereby forming the UHI effect (Trần Thị Vân, 2010). This phenomenon is characterized by significantly higher temperatures in urban areas compared to nearby rural regions, primarily due to human activities (Solecki et al., 2004). A key cause of UHI is the reduction of vegetative cover and the replacement of natural surfaces with impervious artificial materials, which decreases evapotranspiration into the atmosphere (EPA, 2008). In addition, heat emissions from energy consumption also play a considerable role in this phenomenon (Li & Zhao, 2012). As urban centers grow and expand, average local temperatures tend to rise, leading to the widespread use of the term "urban heat island" in meteorological and environmental studies (Glossary of Meteorology, 2019).

Globally, numerous studies have applied remote sensing and Geographic Information Systems (GIS) in urban spatial analysis and the assessment of the Urban Heat Island (UHI) effect. Among these, Masek et al. (1998) used Landsat satellite imagery to analyze land cover changes in urban areas across the United States, revealing a clear relationship between the expansion of built-up areas and the decline in vegetation cover. Subsequently, the USGS (1999), through its Land Cover Trends program, emphasized the role of remote sensing data in monitoring large-scale urban development. Zhang and Guindon (2005) developed

a method integrating SPOT and Landsat imagery to create detailed urban land use maps, thereby assessing the environmental impacts of development activities on urban areas.

Regarding the spatial characteristics and extent of UHI impacts, Rosenzweig et al. (2006) in New York City identified that areas with high building density and limited green space tend to experience significantly higher temperatures during summer. Meanwhile, Zhou et al. (2014) demonstrated that the conversion of agricultural or natural land into built-up areas leads to a marked increase in urban surface temperatures, particularly at night and during the summer season. Li et al. (2019) also revealed a strong upward trend in the UHI phenomenon in major cities across Asia and Africa, where climate change combined with rapid urbanization has led to the emergence of "mega urban heat islands."

To cope with this phenomenon, Santamouris (2014) reviewed 80 studies and concluded that solutions such as green roofs, the use of reflective materials, and the expansion of green spaces can help reduce surface temperatures by 1 to 4°C. Bowler et al. (2010), through an analysis of 38 studies, also confirmed the significant role of green spaces and water bodies in lowering average urban air temperatures by 0.9°C to 4.0°C. Gartland (2008), in the book *Heat Islands: Understanding and Mitigating Heat in Urban Areas*, proposed various urban design solutions to mitigate UHI, including the use of appropriate building materials, improved ventilation, and increased tree planting. In addition, Stone et al. (2010) emphasized that areas heavily affected by UHI often experience higher heat-related mortality rates and greater energy consumption, particularly in tropical urban areas.

In Vietnam, the application of remote sensing technology to study urban issues has been implemented in many major cities. In Hanoi, Pham Ngoc Dang et al. (2000) used satellite imagery to assess the relationship between the degree of concretization and the Urban Heat Island (UHI) phenomenon, revealing a rapid increase in surface temperature in central urban districts. Pham Bach Viet (2008) expanded on this research by combining MODIS and Landsat images to produce thermal maps and identify high-risk areas affected by UHI, proposing the reorganization of green space planning. In Ho Chi Minh City, Tran Thi Van et al. (2011a) evaluated land cover changes from 1990 to 2010, indicating a sharp decline in green spaces and water surfaces alongside the expansion of residential and industrial areas. In another study (2011b), the authors analyzed surface temperature using Landsat imagery and recorded a temperature difference between central and suburban areas of up to 5–7°C during the dry season. Luong Van Viet and Vu Thanh Ca (2010) emphasized that rapid urbanization in Ho Chi Minh City is disrupting ecological spatial balance, increasing the risk of flooding and environmental pressure. Son et al. (2017) applied a statistical analysis method in combination with Landsat imagery to monitor UHI trends over 20 years and evaluated the relationship with the NDVI index. In Da Nang City, Dang Trung Tu (2015) used Landsat imagery and GIS data to assess land use changes and surface temperature, finding that areas with the highest construction rates also experienced the most rapid surface temperature increases. More recently, a study by Nguyen Kieu Diem (2022) in Can Tho City showed that newly developed urban areas with dense construction had significantly higher surface temperatures than agricultural zones or areas with abundant greenery, also highlighting a negative correlation between NDVI and surface temperature. The study by Phan Truong Khanh (2023) demonstrated that surface temperatures in central areas were significantly higher than in peripheral zones—clearly delineating the urban heat island zone in Long Xuyen City. Regression analysis confirmed a negative relationship between NDVI and Land Surface Temperature (LST) the more greenery, the lower the temperature.

These studies demonstrate that the application of remote sensing imagery in urban heat analysis is an effective tool not only for assessing the current situation but also as a basis for proposing sustainable urban planning solutions, especially in the context of climate change and rapid urbanization in Vietnam. Chau Doc City, An Giang Province, plays a strategic role in socio-economic development, national defense, and trade in the Southwest border region (An Giang Provincial People's Committee, 2020). Urbanization here accelerated rapidly since the 1990s, with Chau Doc upgrading from a Grade IV town (1999) to Grade III (2007), and becoming a provincial city in 2013 (An Giang Department of Construction, 2015). This development was driven by infrastructure projects such as lighting systems, solid housing (Nguyen & Tran, 2003), the 2,000-hectare flood-surpassing residential cluster in Tinh Bien – Chau Doc (Southern Institute of Water Resources Science, 2002), and transport and public works like Vinh Nguon Bridge and the central park (An Giang Newspaper, 2011). Simultaneously, water and

electricity supply systems, main roads, and tourism infrastructure such as the road up Sam Mountain were upgraded to improve living conditions, transportation, and attract tourism (An Giang Department of Construction, 2017; Chau Doc City People's Committee, 2018; An Giang Department of Transport, 2019). Between 2010 and 2015, more than 280 projects with a total investment exceeding 2,200 billion VND were allocated to industry, commerce, services, and infrastructure (Chau Doc City People's Committee, 2015). Cultural and tourism works like the 18-meter-tall Buddha statue contributed to expanding urban space and strengthening regional linkage (An Giang Department of Tourism, 2016). From 2021 onwards, key projects such as the Tan Chau – Chau Doc route, Chau Doc Bridge, and Vinh Nguon border gate economic zone continue to create breakthroughs for urban development (An Giang Newspaper, 2023).

Temperature surveys in Chau Doc city show that the urban center area has temperatures higher by 1.5 to 3°C compared to the outskirts, clearly reflecting the Urban Heat Island (UHI) phenomenon. This phenomenon is similar to other tropical humid climate cities such as Bangkok (Phuichit & Kaneko, 2018) and Ho Chi Minh City (Nguyen & Nguyen, 2015).

The study of urban spatial structure, particularly the distribution of areas with different building densities, green spaces, water bodies, along with meteorological factors, plays a crucial role in creating urban thermal maps and identifying zones heavily affected by the Urban Heat Island (UHI) effect. This scientific basis is essential for proposing planning solutions such as increasing green spaces, expanding water surfaces, and using environmentally friendly construction materials to mitigate UHI, improve living environment quality, and adapt to climate change (Santamouris, 2015; Emmanuel & Loconsole, 2015).

Based on this importance, this study was conducted to assess the current status and variations of the Urban Heat Island (UHI) effect in Chau Doc City during the period 2014–2022. Specifically, the study developed land use/land cover maps based on the NDVI index for the years 2014, 2018, and 2022, and simultaneously established corresponding land surface temperature (LST) maps for these three time points. Through this, data on the area of various land cover types (such as residential areas, green spaces, and water bodies) were extracted, combined with secondary data on building density and field-observed surface temperature measurements to evaluate the accuracy and effectiveness of the image interpretation process. This study aims to address the following questions: (1) How do the surface temperature values estimated from satellite images differ from direct field observations? (2) Is there a difference in surface temperature between the urban core and suburban areas or zones with high vegetation density? (3) Has the increase in urbanization over time significantly raised surface temperatures between the years 2014, 2018, and 2022? (4) Is the correlation between the NDVI vegetation index and surface temperature in the two study areas linear and reliable?

2. METHODOLOGY

2.1 Characteristics of the Study Area

Chau Doc City is located on the banks of the Hau River, about 210 km west of Ho Chi Minh City, approximately 115 km from Can Tho City, and around 55 km northwest of Long Xuyen City along National Highway 91. Chau Doc City has the following administrative boundaries: To the north, it borders An Phu District and the border with Cambodia. To the east, it borders Phu Tan District and Tan Chau Town. To the south, it borders Chau Phu District. To the west, it borders Cambodia. To the southwest, it borders Tinh Bien District. Situated right on the border between Vietnam and Cambodia, Chau Doc is currently classified as a Class II city. The population of Chau Doc is concentrated along the Hau River, near National Highway 91, in the central wards of the city, and in residential areas, with a young demographic structure and an urban population accounting for nearly 80%.

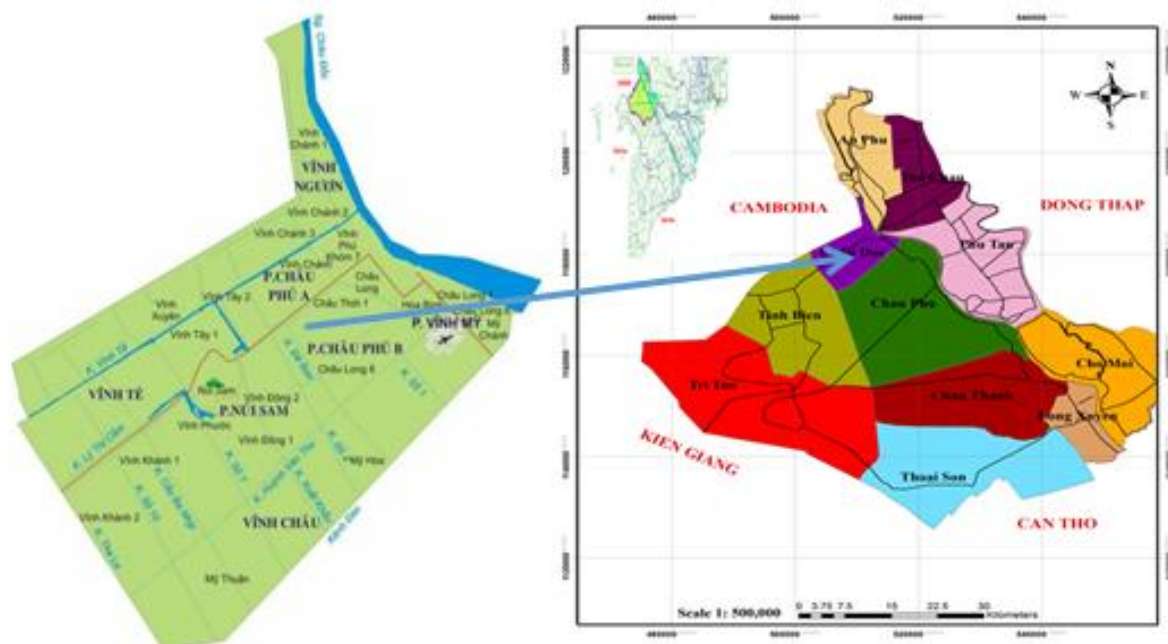


Figure 1: Map of Chau Doc City

2.2 Landsat image data

The satellite image data used in this study are Level 1A processed LANDSAT 8 OLI images with a spatial resolution of 30 meters, using the UTM projection system (WGS 84), zone 48. The images were acquired on dry-season dates: March 17, 2014 (OLI); **March 12, 2018 (OLI)**; and February 19, 2022 (OLI), all with low cloud cover (<10%), allowing for clear differentiation of surface land cover features.

Table 1. Landsat 8 Image Information

Spectral Band	Wavelength (μm)	Resolution
1	0.433–0.453	30 m
2	0.450–0.515	30 m
3	0.525–0.600	30 m
4	0.630–0.680	30 m
5	0.845–0.885	30 m
6	1.560–1.660	30 m
7	2.100–2.300	30 m
8	0.500–0.680	15 m
9	1.360–1.390	30 m
10	10.6–11.2	100 m
11	11.5–12.5	100 m

2.3 Remote sensing image processing and Land cover classification

The Landsat images were pre-processed to enhance clarity, including image sharpening, band combination, preliminary cropping, and geometric correction transforming the scanned images from pixel-based row and column coordinates to real-world geographic coordinates.

Subsequently, ERDAS software was used to generate the Normalized Difference Vegetation Index (NDVI) images. The vegetation index was calculated using the following formula (Tucker, 1979):

$$NDVI = \frac{(\text{Band NIR} - \text{Band RED})}{(\text{Band NIR} + \text{Band RED})} \quad (1)$$

Where: NIR is the Near Infrared band; RED is the red visible light band. For Landsat 8, BLUE corresponds to Band 2; RED is Band 4, NIR is Band 5, and SWIR corresponds to Bands 6 and 7.

The NDVI (Normalized Difference Vegetation Index) ranges from -1 to 1. Negative values typically indicate surfaces such as clouds, water, snow, or areas with high reflectance in the visible spectrum. Values between 0 and 0.1 usually represent bare soil, rocks, or built-up areas. Positive values indicate vegetation cover, and as vegetation density increases, NDVI values also increase. Typically, an NDVI value below 0.1 suggests sparse vegetation in the area.

2.4 The estimation of Land Surface Temperature (LST)

The estimation of Land Surface Temperature (LST) from satellite imagery involves a multi-step process using thermal infrared bands. In this study, LST was estimated from Landsat 8 OLI/TIRS data through the following steps:

Step 1: Conversion of Digital Numbers (DN) to Top of Atmosphere Radiance (TOA): The thermal band (Band 10) of Landsat 8 is converted from DN values to TOA spectral radiance using the radiance re-scaling factors provided in the metadata (MTL file) using the formula (USGS, 2016):

$$L_{\lambda} = M_L \times Q_{cal} + A_L \quad (2)$$

Where: L_{λ} is the TOA spectral radiance ($W/(m^2 \cdot sr \cdot \mu m)$); M_L is the radiance multiplicative scaling factor. A_L is the radiance additive scaling factor. Q_{cal} is the quantized and calibrated standard product pixel value (DN)

Step 2: Conversion to Brightness Temperature (BT): TOA radiance is then converted to Brightness Temperature (BT) in Kelvin using the following formula:

$$BT = K2 / \ln [(K1/L_{\lambda}) + 1] \quad (3)$$

Where: BT is the brightness temperature in Kelvin; $K1$, $K2$ are calibration constants from the metadata are calibration constants from the metadata.

Step 3: Estimation of Land Surface Emissivity (LSE): LSE is estimated using NDVI values derived from OLI bands. Based on NDVI thresholds, emissivity values are assigned depending on land cover types (e.g., vegetation, bare soil, built-up).

Step 4: Calculation of Land Surface Temperature (LST): Finally, LST is calculated using the following formula (Gupta, 1991):

$$LST = \frac{BT}{\left(1 + \left(\frac{\lambda \times BT}{c_2}\right) \times \ln(LSE)\right)} \quad (4)$$

Where: λ is the wavelength of emitted radiance ($\approx 10.895 \mu m$ for Landsat 8 Band 10); $c_2 = (hc_1)/\sigma = 1.438 \times 10^{-2} m \cdot K$; LSE is the land surface emissivity; h is Planck's constant ($6.626 \times 10^{-34} J \cdot s$); c_1 is the speed of light ($2.998 \times 10^8 m/s$). σ is Boltzmann's constant ($1.38 \times 10^{-23} J/K$); LST values are often converted from Kelvin to Celsius by subtracting 273.15 for easier interpretation.

2.5 Error Assessment Method

Error (%) is the process of determining the degree of deviation between actual measured values and interpreted or predicted values. It helps assess the accuracy of the method by calculating the average deviation. The error formula commonly used to evaluate the suitability of land surface temperature estimation methods is as follows:

Error (%) = [(Observed value – Estimated value) / Observed value] \times 100 (5) This formula provides a percentage that represents how much the estimated value deviates from the observed value, offering insight into the reliability of the estimation method.

3. RESULTS

3.1 Analysis of land cover change through NDVI index

The results of interpreting Landsat satellite images from the years 2014, 2018, and 2022 show that the surface of Chau Doc City is divided into four main land cover categories based on the Normalized Difference Vegetation Index (NDVI) values. NDVI is an index that reflects the greenness of vegetation and plays an important role in assessing the urban environment, particularly in relation to the Urban Heat Island (UHI) effect.

The water surface class has NDVI values ranging from -0.133 to 0.206, indicating strong absorption of near-infrared radiation and reflection of red light, which is characteristic of rivers, ponds, lakes, and canals. The low or negative NDVI values of water surfaces reflect an almost zero photosynthetic capacity. The built-up area class (including residential areas, roads, industrial zones, etc.) has NDVI values ranging from 0.198 to 0.331. This group has little or no vegetation cover and typically exhibits high surface temperatures due to solar radiation absorption, contributing to the Urban Heat Island (UHI) effect in central urban areas.

The rice field class has NDVI values ranging from 0.280 to 0.447, indicating a moderate level of greenness that varies depending on the stages of sowing, growth, and harvest. When rice plants are in a vigorous

growth phase, NDVI values are higher; conversely, during the dry season or after harvest, the values decrease. The vegetation class (including perennial crops, gardens, plantations, urban parks, etc.) has the highest NDVI values, ranging from 0.360 to 0.630. These areas have dense vegetation with strong photosynthetic activity, playing a crucial role in regulating the local microclimate, reducing surface temperature, and creating "cool zones" within the urban landscape (Figures 2, 3, 4, and 5).

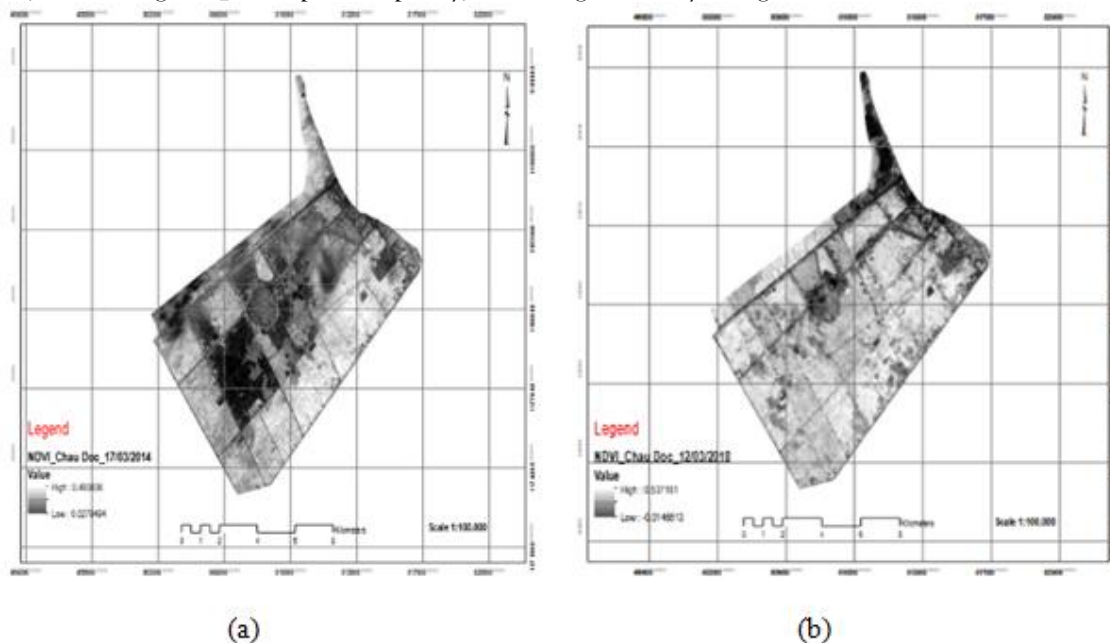
Analysis of the 2022 satellite imagery data shows that the total interpreted surface area of Chau Doc City is 10,332.30 hectares, achieving an accuracy rate of 98.18% compared to the official statistics (10,523.11 hectares) published by the Department of Natural Resources and Environment of An Giang Province. This minor discrepancy indicates a high level of reliability in the remote sensing image analysis method for determining current land use status.

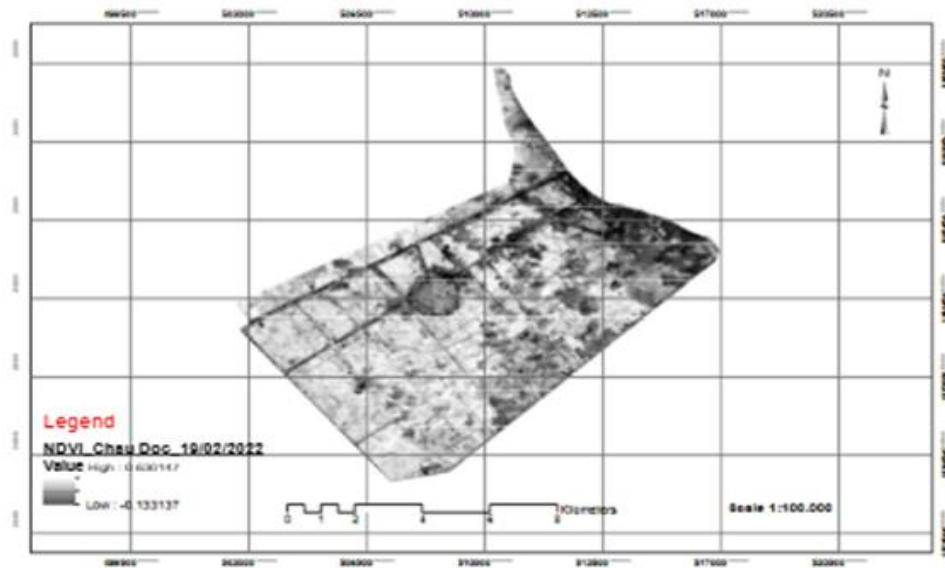
One of the most notable features during the study period is the rapid increase in built-up area. In 2022, the area of constructed zones reached 3,232.15 hectares, marking a 57.5% increase compared to 2014 (1,372.31 hectares). This change is clearly illustrated in Figures 3 and 5, demonstrating the expansion of urban space and infrastructure over the eight-year period. This trend reflects the strong urbanization process and the development of infrastructure systems to meet the growing population's needs, including the expansion of residential areas, commercial centers, educational and healthcare facilities, and public infrastructure.

In contrast, during the same period, two traditional land cover types water surface and rice fields showed a significant decline. Specifically, the water surface area decreased by 33.04% compared to 2014, while the rice field area decreased by 18.7%. This decline reflects the conversion of land use from agricultural and water management purposes to urban land, serving construction and non-agricultural activities. This is a common trend in developing urban areas, where the increasing demand for residential and infrastructure space leads to a reduction in traditional agricultural land. However, this also poses challenges to food security, water resource management, and the preservation of urban ecological landscapes.

Notably, despite rapid urbanization, the green space area in Chau Doc City remained stable during the 2014–2022 period. This indicates a certain level of commitment by local authorities to environmental protection and green space development.

Maintaining green space plays a vital role in: Improving air quality; Mitigating the Urban Heat Island effect; Enhancing CO₂ absorption capacity; Providing a healthy living environment for residents.





(c)

Figure 2. NDVI value maps of Chau Doc City on March 17, 2014 (a), March 12, 2018 (b), and February 19, 2022 (c).

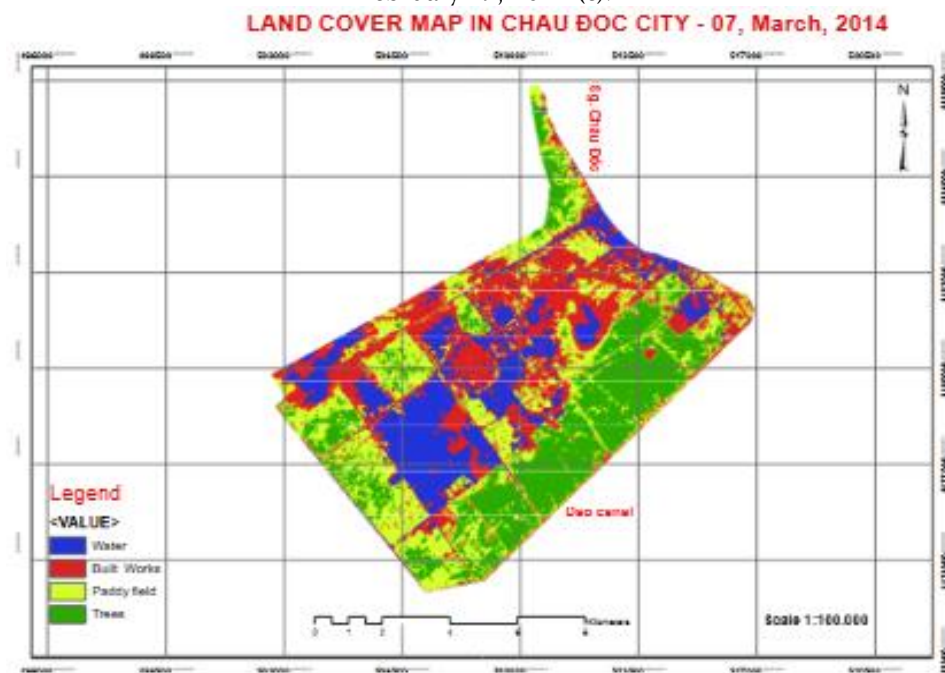


Figure 3. Land cover distribution map of Chau Doc City on March 17, 2014.

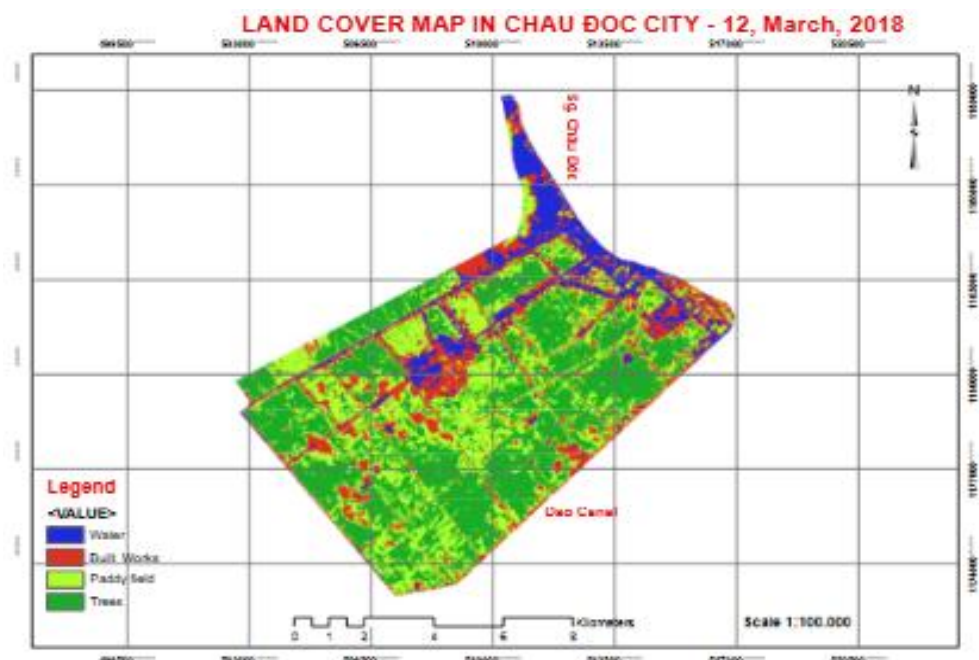


Figure 4. Land cover distribution map of Chau Doc City on March 12, 2018.

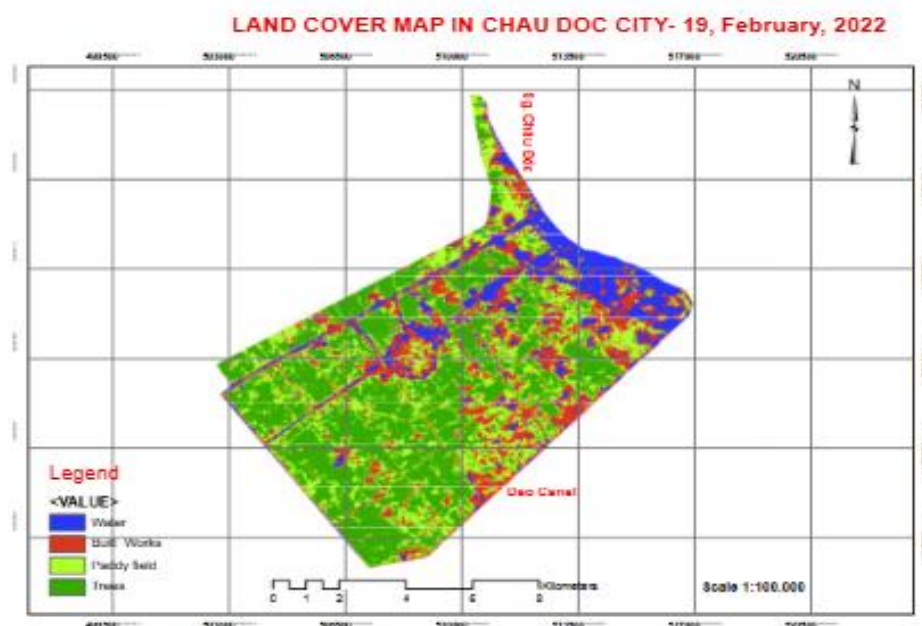


Figure 5. Land cover distribution map of Chau Doc City on February 19, 2022.

In summary, data from the 2022 satellite imagery provides a comprehensive overview of land use changes in Chau Doc City (Table 2). The significant increase in built-up areas alongside the decline in water bodies and rice fields reflects the process of urbanization and land use conversion. However, the stable maintenance of green space indicates that the city still prioritizes environmental factors during its development. These changes not only reflect economic growth but also present challenges and opportunities for sustainable management and development of the city in the future.

Table 2. Interpretation Results of Surface Cover Area in Chau Doc City at the acquisition dates of 2014, 2018, and 2022,

❖ Objects	❖ Area (ha) ❖ 17/03/2014	❖ Area (ha) ❖ 12/03/2018	❖ Area (ha) ❖ 19/02/2022
❖ Water	❖ 5.977,12	❖ 5.403,69	❖ 4.492,81
❖ Built-up area	❖ 1.372,31	❖ 2.354,75	❖ 3.232,15

❖ Paddy field	❖ 2.340,96	❖ 2.099,18	❖ 1972,19
❖ Trees	❖ 643,39	❖ 656,35	❖ 635,15
❖ Total	❖ 10.333,78	❖ 10.333,15	❖ 10.332,30

3.2 Green Space Per Capita Index and Its Impact on Land Surface Temperature (LST) in Chau Doc City

3.2.1 Green Space Per Capita Index

The **green space per capita index** is considered an important composite indicator that reflects the balance between socio-economic development and environmental protection in urban areas. A high value of this index not only demonstrates the local government's commitment to improving the quality of life but also contributes to improving the microclimate, reducing air pollution, creating recreational spaces for residents, and supporting urban biodiversity. Calculations based on spatial and demographic data show that: In **2014**, the green space per capita was **57.91 m²/person**. By **2018**, this index had increased to **63.86 m²/person**, reflecting the city's efforts to expand and maintain green spaces through activities such as planting new trees, renovating parks, and integrating ecological elements into urban planning. However, in **2022**, the index declined to **56.95 m²/person**.

This decrease may be attributed to several factors, including: Population growth due to in-migration. Land use conversion from green space to built-up areas for urban development, Loss of green areas due to infrastructure construction, Lack of adequate planning for green space conservation.

Despite the slight decline, this value still far exceeds the public green space standard defined in **TCVN 9257:2012** (ranging from **20.4 to 24.5 m²/person** for type I and II urban areas). However, it is important to note that in this study, green space area was calculated based on total vegetation cover in the city, including public urban greenery, orchards, and private green areas, while TCVN standards only account for public green space (such as streets, parks, and flower gardens). Maintaining a high level of green space indicates that: The **living environment quality in Chau Doc** is at a good level, contributing to the **mitigation of the urban heat island (UHI) effect**, It enhances **property values**, **attracts ecotourism**, and contributes to the image of a **modern, ecological urban area**, It reflects the **success of local authorities in urban management and sustainable development planning**.

3.2.2 Land Surface Temperature (LST) Variation (Land Surface Temperature – LST).

Changes in urban surface cover due to infrastructure development and land-use conversion have a clear impact on land surface temperature (LST)—a key factor in assessing the Urban Heat Island (UHI) effect. Analysis of satellite imagery from the years 2014, 2018, and 2022 reveals the following: LST values across the study area range from 20.26°C to 38.84°C (Figures 6, 7, and 8). The highest LST values are typically found in central wards, production zones, markets, industrial areas, and asphalt-paved roads—areas characterized by high building density and low vegetation cover. These areas are classified as SUHI-2, with LST ranging from 31.42°C to 38.84°C. In contrast, areas with dense vegetation and low population density (SUHI-4) show lower LST values, ranging from 20.26°C to 29.81°C. Water surfaces (SUHI-1) exhibit LST values ranging from 29.46°C to 33.43°C, while rice paddy fields (SUHI-3) show LST between 26.41°C and 31.34°C. The average LST values at the time of satellite image acquisition in each year are as follows: in 2014: 29.56°C ± 2.10; in 2018: 30.27°C ± 1.52; in 2022: 29.43°C ± 1.23. These results show that LST in 2022 slightly decreased compared to 2014 (by -0.13°C) and 2018 (by -0.84°C). The decreasing standard deviation over the years indicates a trend toward more stable microclimatic conditions in the urban area. This stabilization can be attributed to: The consistent maintenance of high green space coverage, which has helped mitigate increases in LST despite population growth and urban expansion. The strategic distribution of green spaces and climate-regulating elements such as lakes and parks, which have contributed to microclimate stability in residential areas. The LST frequency distribution is shown in Figure 9. The x-axis represents land surface temperature values (°C). The y-axis shows the frequency of each temperature range—that is, the number of pixels with LST values falling within each respective range.

The chart for 2014 (Figure 9a) displays a slightly right-skewed bell-shaped distribution, indicating an asymmetrical spread of LST values. The peak frequency (~6,500 pixels) falls around 28.3°C, representing

the dominant land cover type in Chau Doc in 2014, primarily agricultural areas, water surfaces, forests, and ecological zones. The maximum LST values reaching up to 36.4°C reflect the presence of high-temperature zones, likely the urban center. Compared to subsequent years, 2014 exhibited more stable temperatures with less pronounced signs of the Urban Heat Island (UHI) effect, making it an important baseline for evaluating urban warming trends.

The chart for 2018 (Figure 9b) shows a right-skewed normal distribution, meaning most of the city had LST values between 28°C and 31°C. The mode (the most frequent temperature range) accounts for approximately 70–80% of the urban area.

These areas generally include Medium-density residential zones; Areas with partial vegetation cover such as rice fields or fruit orchards; Semi-urban areas.

Zones experiencing strong UHI effects—within the temperature range of 33.45°C to 38.83°C—appear less frequently but are still clearly present. These areas are typically found in: The city center; Major transportation corridors; Industrial, commercial, or large marketplace areas.

The chart for 2022 (Figure 9c) shows that the LST range of 28–31°C overwhelmingly dominates, indicating that most areas in Chau Doc have good vegetation cover and moderate building density. The 2022 LST chart reflects that the majority of the city's land surface falls within the medium to low-temperature range, centered around 28–30°C. Around 70–80% of the urban area is not strongly affected by the UHI effect, demonstrating the effectiveness of green space planning and appropriate land cover distribution.

However, some areas still exhibit LST values above 31.5°C (SUHI-2). Compared to data from 2014 and 2018, the LST range in 2022 is narrower and more evenly distributed. This indicates greater stability in the urban microclimate, likely resulting from green space planning policies or effective building density control.

By combining the information in Figure 9 with the previously described SUHI data, the 2022 LST can be categorized as follows:

Table 3. Spatial Distribution of Surface Urban Heat Island

SUHI region	Temperature range (°C)	Characteristics
SUHI-4	25 – 28°C	Agricultural areas, green spaces, and wetlands.
SUHI-3	28 – 30.56°C	Rice fields, low-density residential areas
SUHI-1	30.56 – 31.43°C	Water bodies, peri-urban areas
SUHI-2	31.43 – 37.31°C	Urban center, concrete surfaces, paved roads.

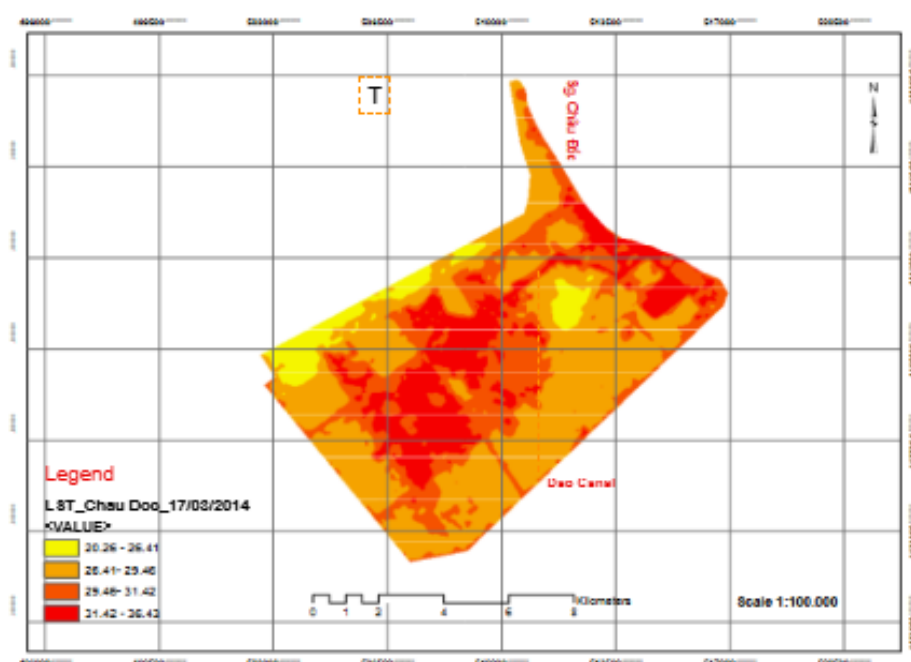


Figure 6. Spatial distribution of LST (°C) in Chau Doc City, based on Landsat data on March 17, 2014.

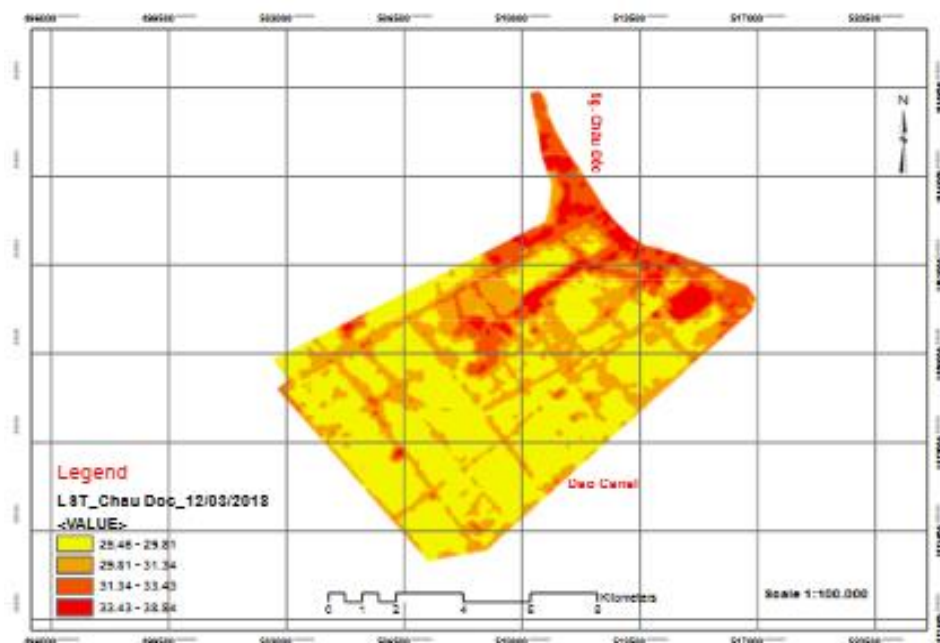


Figure 7. Spatial distribution of LST (°C) in Chau Doc City, based on Landsat data for March 12, 2018.

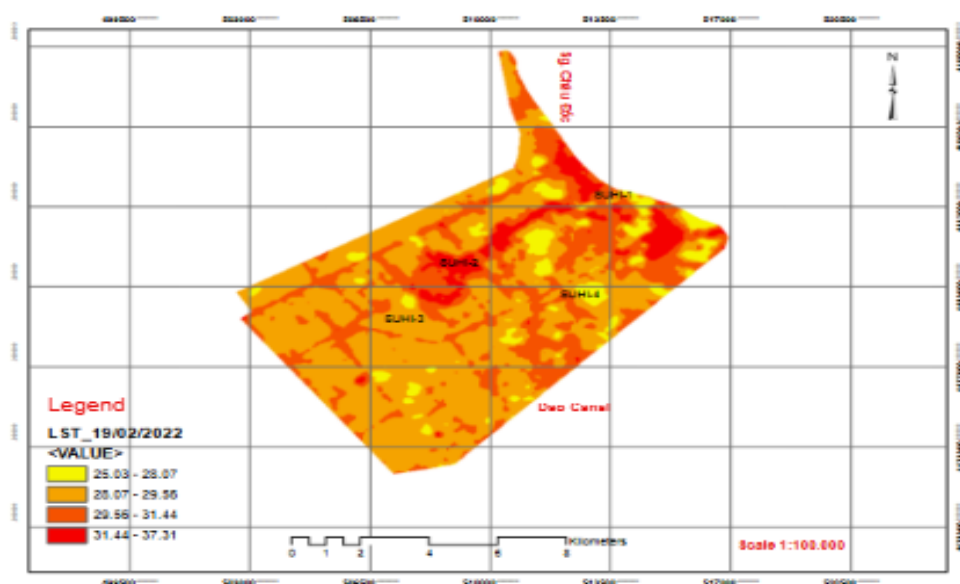


Figure 8. Spatial distribution of LST (°C) in Chau Doc City on February 19, 2022.

The results of the interpreted LST (°C) distribution from satellite images of the city were also validated by measuring the temperature of various objects: water surfaces, buildings and houses, roads, bridges, industrial zones, rice fields, and green areas during January, February, and March at 244 field points (Figure 10). The results show that the error between the measured temperature and the interpreted values ranged from 3.21% to 10.7%, with an average deviation of $\pm 2.9^{\circ}\text{C}$ compared to actual measurements (Table 4).

Bảng 4 Percentage difference between Surveyed LST values (19. Feb, 2022) and satellite-derived LST estimates.

Survey location	Surveyed average LST value (°C)	Estimated average LST value (°C)	Error (%)
SUHI -1	28,96	29,89	3,21
SUHI - 2	31,15	28.52	8,44
SUHI -3	30,75	28.77	6,44

SUHI -4	37,83	33.78	10,7
Average LST value	32.42	29,43	9,22

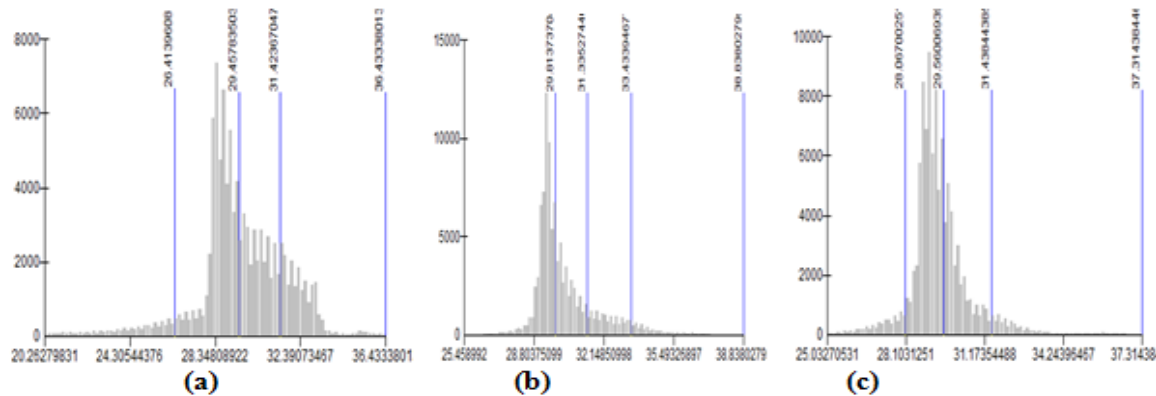


Figure 9. Frequency distribution of LST (°C) ranges at acquisition dates in 2014 (a), 2018 (b), and 2022 (c) for Chau Doc City.



Figure 10. Surface Cover Temperature in Chau Doc City in 2022

3.3 Correlation between NDVI and Land surface temperature (LST) in Chau Doc City

At the acquisition dates of 2014, 2018, and 2022, the relationship between LST and NDVI was consistently linear with a negative slope (Figures 11, 12, and 13). This inverse relationship indicates that areas with dense and healthy vegetation cover (high NDVI values) typically exhibit lower land surface temperatures. This reflects the cooling effect of vegetation through processes such as evapotranspiration, shade provision, and heat absorption, suggesting a healthier and more ecological environment.

Figure 11 illustrates the correlation between Land Surface Temperature (LST) and the Normalized Difference Vegetation Index (NDVI) in Chau Doc City in 2014. The analysis results show an inverse relationship between NDVI and LST, expressed through the linear regression equation: $LST = -9.2445 \times NDVI + 32.187$, with a correlation coefficient $R = 0.385$. The negative slope (-9.2445) implies that for every 0.1 unit increase in NDVI, the land surface temperature tends to decrease by approximately 0.92°C .

This underscores the significant role of vegetation cover in regulating ambient temperature through mechanisms such as shading from solar radiation and enhancing evapotranspiration. However, with a moderate correlation coefficient ($R = 0.385$), it is evident that besides NDVI, other factors also influence land surface temperature, such as surface material types, building density, topography, and urban microclimate characteristics. These results suggest that increasing green space and vegetation coverage in urban planning can play a crucial role in mitigating the Urban Heat Island (UHI) effect and adapting to climate change.

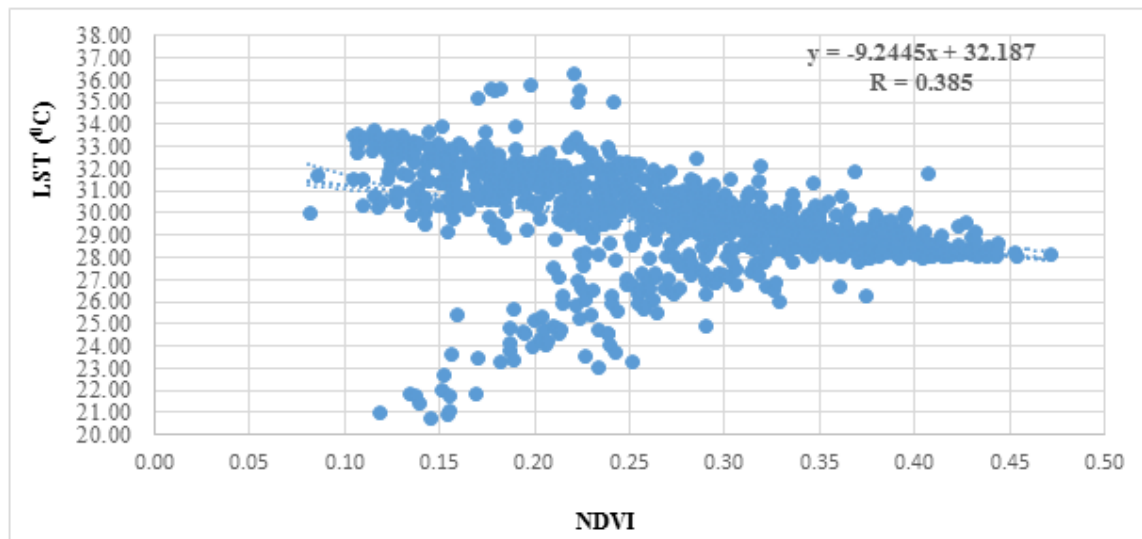


Figure 11. Correlation between LST and NDVI in Chau Doc City on March 17, 2014.

Figure 12 illustrates the correlation between Land Surface Temperature (LST) and the Normalized Difference Vegetation Index (NDVI) in Chau Doc City on March 12, 2018. The results reveal a relatively strong negative relationship between the two variables, described by the linear regression equation: $LST = -11.227 \times NDVI + 34.178$, with a correlation coefficient of $R = 0.687$. The steep negative slope (-11.227) indicates that for every 0.1 unit increase in NDVI, the average surface temperature tends to decrease by approximately 1.12°C . This is a clear indication of vegetation's role in regulating temperature, especially in the context of urbanization. The high correlation coefficient ($R=0.687$) reflects a strong link between vegetation cover and surface temperature variation, emphasizing the importance of green spaces in mitigating the **Urban Heat Island (UHI)** effect. Additionally, compared to 2014, the relationship between NDVI and LST in 2018 is stronger, suggesting that changes in land use structure or vegetation cover density may have positively influenced surface temperature conditions in the study area.

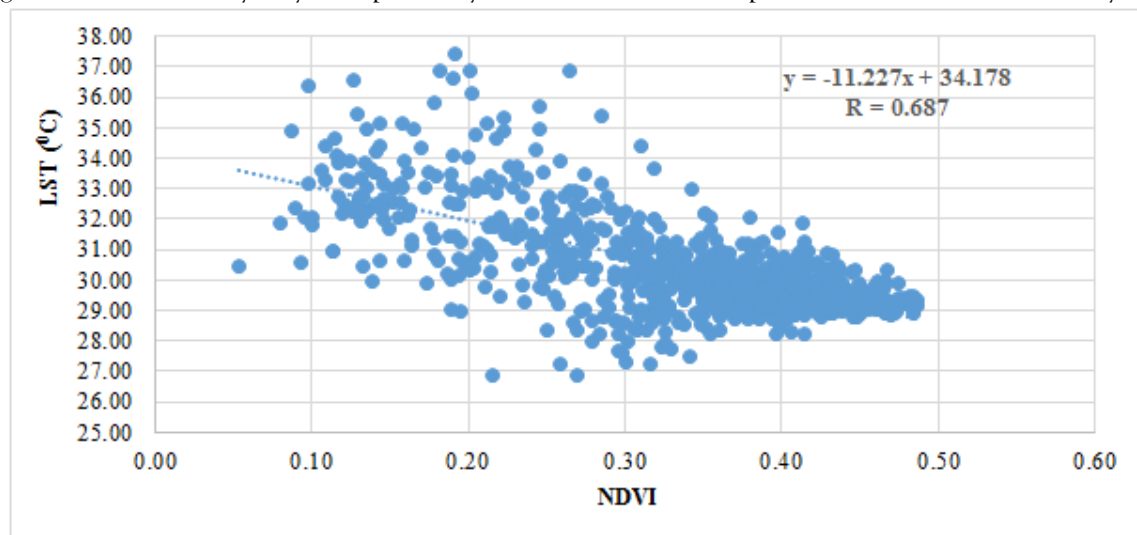


Figure 12. Correlation between LST and NDVI in Chau Doc City on March 12, 2018.

Figure 13 illustrates the correlation between Land Surface Temperature (LST) and the Normalized Difference Vegetation Index (NDVI) at the acquisition date of February 19, 2022. Although the linear regression equation shows a decreasing trend of temperature with increasing NDVI, specifically: $LST = -2.433 \times NDVI + 30.363$, the correlation coefficient of $R=0.264$ indicates a weak relationship between the two variables. The small negative slope (-2.4331) suggests that when NDVI increases by 0.1 units, LST only decreases by approximately 0.24°C —a very limited effect. This result indicates that in 2022, the cooling effect of

vegetation in Châu Đốc City had significantly diminished compared to previous years such as 2014 ($R=0.385$) and especially 2018 ($R=0.687$).

This decline may be attributed to a reduction in vegetation density or an increase in anthropogenic factors (e.g., urban concrete surfaces, expansion of built-up areas), which weaken the cooling influence of urban green spaces. These findings highlight the urgent need for policies aimed at protecting and expanding green cover, particularly in the context of climate change and the increasing severity of the Urban Heat Island (UHI) phenomenon.

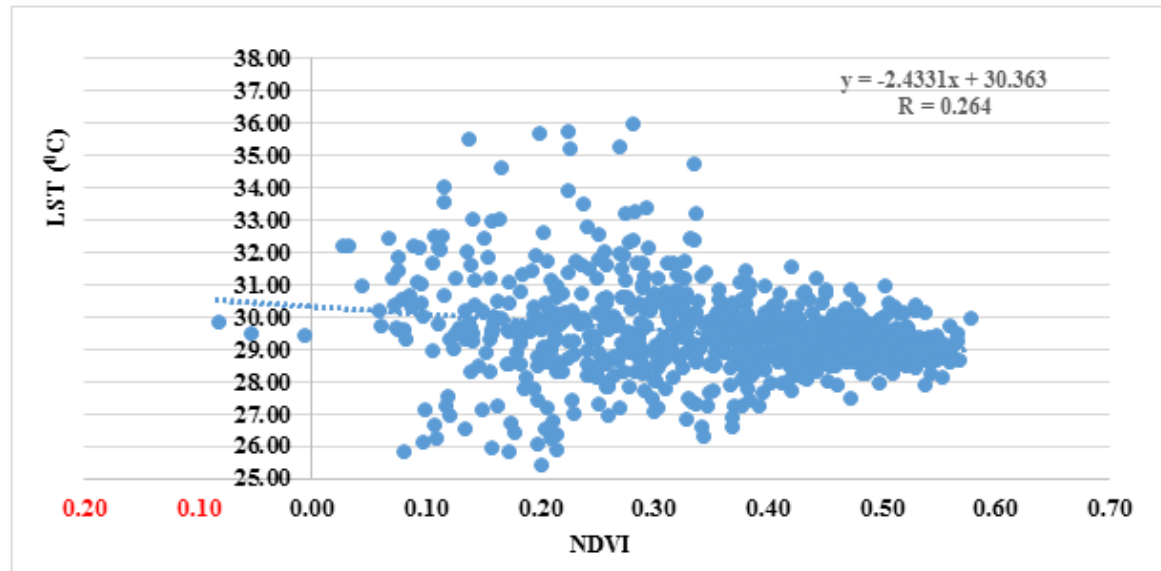


Figure 13. Correlation between LST and NDVI in Chau Doc City on February 19, 2022

4. CONCLUSIONS AND RECOMMENDATIONS

4.1. Conclusions

The study conducted a comprehensive assessment of the relationship between the Normalized Difference Vegetation Index (NDVI) and Land Surface Temperature (LST) in Châu Đốc City during the period 2014–2022, combined with an analysis of thermal frequency maps to clarify the spatiotemporal trends of the Urban Heat Island (UHI) phenomenon. Key highlights include:

❖ NDVI–LST correlation equation

The linear correlation equations show an inverse relationship between NDVI and LST, meaning that the greener the vegetation, the lower the surface temperature.

The year 2018 recorded the strongest correlation coefficient of $R = 0.687$ with a steep slope of -11.227 , demonstrating the significant role of vegetation in regulating temperature.

However, by 2022, the correlation coefficient dropped to $R = 0.264$ and the slope decreased to -2.433 , indicating a marked decline in the cooling effect of vegetation.

New finding: This serves as evidence of the degradation in the quality or area of vegetation cover, likely caused by rapid urbanization and a lack of policies protecting green spaces.

❖ Fluctuations of Land Surface Temperature (LST)

The average land surface temperature (LST) has slightly increased over the years. Hot spots ($LST > 34^{\circ}\text{C}$) have become more frequent and are concentrated in the inner city areas with high building density.

The maximum temperature tends to rise, while the minimum temperature remains relatively stable, resulting in a larger temperature range, which negatively affects health and the urban microclimate.

New finding: The downtown area of Châu Đốc City is becoming a concentrated heat zone, increasing the risk of localized urban heat island effects if no intervention measures are implemented.

❖ Temperature frequency map

The temperature frequency map (especially in 2018) shows an uneven spatial distribution of heat. Some areas exhibit clusters of high temperatures ($> 33^{\circ}\text{C}$) with high frequency, indicating an imbalance in the distribution of green spaces.

By 2022, the frequency of locations with $LST > 32^{\circ}\text{C}$ increased, leading to an expansion of hot zones towards the suburban areas.

New finding: Areas previously considered “thermal buffer zones” (urban fringes or green areas) are gradually warming up, indicating the spread of the urban heat island effect from the city center to the outskirts.

4.2 Recommendations

Based on the above findings, the study proposes the following recommendations: Strengthen the protection and expansion of urban green spaces, especially in areas with a high frequency of elevated temperatures, through the planning of parks, green corridors, and vegetative belts.

Regularly apply remote sensing technology to monitor LST and NDVI, supporting land use planning, management, and mitigation of urban climate change impacts.

Integrate the “urban heat” factor into comprehensive planning strategies, including the development of green infrastructure, use of heat-reflective building materials, and smart urban design adapted to heat conditions.

Prioritize sustainable development in suburban areas to prevent the spread of urban heat islands into zones that play a role in climate regulation.

Promote community awareness and environmental education to enhance understanding of the importance of green spaces and the impacts of uncontrolled development on living environments.

REFERENCES

1. An Giang Department of Construction. (2015). *Report on urban development status in Chau Doc City*.
2. An Giang Department of Construction. (2017). Urban planning and infrastructure improvement program.
3. An Giang Department of Tourism. (2016). Tourism development strategy of Chau Doc City.
4. An Giang Department of Transport. (2019). Transportation development report
5. An Giang Newspaper. (2011). Central Park and infrastructure development news.
6. An Giang Newspaper. (2023). New projects to boost urban development in Chau Doc.
7. An Giang Provincial People's Committee. (2020). Socio-economic development plan of An Giang Province.
8. Arnfield, A. J. (2003). Two decades of urban climate research: a review of turbulence, exchanges of energy and water, and the urban heat island. *International Journal of Climatology*, 23(1), 1–26.
9. Bowler, D. E., Buyung-Ali, L., Knight, T. M., & Pullin, A. S. (2010). Urban greening to cool towns and cities: A systematic review of empirical evidence. *Landscape and Urban Planning*, 97(3), 147–155.
10. Dang Trung Tu. (2015). Assessment of land use change and surface temperature in Da Nang using remote sensing and GIS. Master's Thesis, Da Nang University.
11. Emmanuel, R., & Loconsole, A. (2015). Green infrastructure as an adaptation approach to tackling urban overheating in the Glasgow Clyde Valley Region, UK. *Landscape and Urban Planning*, 138, 71–86.
12. EPA (U.S. Environmental Protection Agency). (2008). Reducing Urban Heat Islands: Compendium of Strategies.
13. Gartland, L. (2008). Heat Islands: Understanding and Mitigating Heat in Urban Areas. Earthscan.
14. Kimura, F., & Kanda, M. (2006). Climate of Tokyo. In: World Meteorological Organization – World Climate Cities Report.
15. Nguyen & Tran. (2003). Infrastructure development and housing in Chau Doc. *Vietnam Urban Research Journal*.
16. Nguyen & Nguyen. (2015). Urban heat island in Ho Chi Minh City: Assessment and solutions. *Journal of Climate Research*, 17(2), 12–20.
17. Nguyen Kieu Diem. (2022). Assessment of surface temperature and vegetation cover in Can Tho City using remote sensing. *Journal of Geography and Environment*, 25(4), 45–53.
18. Li, D., & Zhao, L. (2012). Effect of human activities and urbanization on urban climate in China. *Climatic Change*, 114(2), 479–492.
19. Li, X., Zhou, Y., Asrar, G. R., Imhoff, M., & Li, X. (2019). The surface urban heat island response to urban expansion: A panel analysis for the conterminous United States. *Science of the Total Environment*, 695, 133780.
20. Luong Van Viet & Vu Thanh Ca. (2010). Impacts of rapid urbanization on ecological balance in Ho Chi Minh City. *Vietnam Journal of Environmental Science*, 5(1), 33–40.
21. Masek, J. G., Lindsay, F. E., & Goward, S. N. (2000). Dynamics of urban growth in the Washington DC metropolitan area, 1973–1996, from Landsat observations. *International Journal of Remote Sensing*, 21(18), 3473–3486.
22. Ng, E., Chen, L., Wang, Y., & Yuan, C. (2012). A study on the cooling effects of greening in a high-density city: An experience from Hong Kong. *Building and Environment*, 47, 256–271.
23. Oke, T. R. (1982). The energetic basis of the urban heat island. *Quarterly Journal of the Royal Meteorological Society*, 108(455), 1–24.
24. Pham Bach Viet. (2008). Application of remote sensing and GIS in urban thermal analysis in Hanoi. Institute of Geography, VAST.
25. Pham Ngoc Dang et al. (2000). Urban surface temperature analysis in Hanoi using satellite imagery. *Journal of Natural Resources and Environment*, 3(2), 15–22.

26. Phan Truong Khanh. (2023). Research on urbanization developments in Long Xuyen city using GIS and remote sensing techniques
27. Phuichit, P., & Kaneko, S. (2018). Urbanization and UHI effect in Bangkok. *Asia-Pacific Journal of Atmospheric Sciences*, 54(4), 479-492.
28. Rosenzweig, C., Solecki, W. D., Parshall, L., et al. (2006). Mitigating New York City's heat island: Integrating stakeholder perspectives and scientific evaluation. *Bulletin of the American Meteorological Society*, 87(2), 193-204.
29. Roth, M., Oke, T. R., & Emery, W. J. (1989). Satellite-derived urban heat islands from three coastal cities and the utilization of such data in urban climatology. *International Journal of Remote Sensing*, 10(11), 1699-1720.
30. Santamouris, M. (2014). On the energy impact of urban heat island and global warming on buildings. *Energy and Buildings*, 82, 100-113.
31. Santamouris, M. (2015). Regulating the damaged thermostat of the cities—Status, impacts and mitigation challenges. *Energy and Buildings*, 91, 43-56.
32. Solecki, W. D., Rosenzweig, C., Parshall, L., et al. (2004). Mitigation of the heat island effect in urban New Jersey. *Environmental Hazards*, 6(1), 39-49.
33. Son, N. T., Thanh, B. X., & Chen, C. F. (2017). Monitoring surface urban heat islands over the Vietnamese metropolitan areas using Landsat data (1995-2015). *Sustainable Cities and Society*, 30, 104-116.
34. Southern Institute of Water Resources Science. (2002). Report on flood-resilient residential cluster in Chau Doc and Tinh Bien.
35. Tran Thi Van. (2010). Urban development and heat island effect in Ho Chi Minh City. *Urban Studies Journal*, 12(4), 56-62.
36. Tran Thi Van et al. (2011a). Land cover change analysis in Ho Chi Minh City using remote sensing. *Vietnam Geographical Science Journal*, 19(2), 88-96.
37. Tran Thi Van et al. (2011b). Surface temperature analysis of HCMC using Landsat images. *Journal of Remote Sensing and Environment*, 7(3), 33-40.
38. USGS (United States Geological Survey). (1999). Land Cover Trends Project. USGS Report.
39. Voogt, J. A., & Oke, T. R. (2003). Thermal remote sensing of urban climates. *Remote Sensing of Environment*, 86(3), 370-384.
40. Zhang, Y., & Guindon, B. (2005). Using satellite data to model and map urban land use and change. *Urban Remote Sensing*, CRC Press.
41. Zhou, D., Zhao, S., Liu, S., Zhang, L., & Zhu, C. (2014). Surface urban heat island in China's 32 major cities: Spatial patterns and drivers. *Remote Sensing of Environment*, 152, 51-61.